Heavy-Organic Particles Deposition from Petroleum Fluid Flow in Oil Wells and Pipelines

Joel Escobedo(*) and **G.Ali Mansoori**(**)
University of Illinois at Chicago
851 S. Morgan St. (M/C 063), Chicago, IL 60607-7052 USA

ABSTRACT

Suspended asphaltenic heavy organic particles in petroleum fluids may stick to the inner walls of oil wells and pipelines. This is the major reason for fouling and arterial blockage in the petroleum industry. This report is devoted to study the mechanism of migration of suspended heavy organic particles towards the walls in oil-producing wells and pipelines. In this report we present a detailed analytical model for the heavy organics suspended particles deposition coefficient corresponding to petroleum fluids flow production conditions in oil wells. We predict the rate of particle deposition during various turbulent flow regimes. The turbulent boundary layer theory and the concepts of mass transfer are utilized to model and calculate the particle deposition rates on the walls of flowing conduits. The developed model accounts for the eddy diffusivity, and Brownian diffusivity as well as for inertial effects.

The analysis presented in this paper shows that rates of particle deposition (during petroleum fluids production) on the walls of the flowing channel due solely to diffusional effects are small. It is also shown that deposition rates decrease with increasing particle size. However, when the process is momentum controlled (large particle sizes) higher deposition rates are expected.

KEYWORDS
Asphaltene, Brownian deposition coefficient, diffusivity, diamondoid, heavy organic particles, paraffin/wax, particle deposition, petroleum fluid, prefouling behavior, production operation, suspended particles, turbulent flow.

(*) Present address: Case Western Reserve University, 10900 Euclid Ave, Cleveland, OH 44106 - E-mail: *joelescobedo1@gmail.com*
(**) Corresponding author - E-mail: *mansoori@uic.edu*

INTRODUCTION

A common problem faced by the oil industry is the deposition of heavy organics inside the production wells, storage vessels, and transfer pipelines. Our studies and experiences have indicated that heavy organic deposition is one of the major factors that increase the cost of production and transportation of petroleum fluids [1, 2]. Furthermore, miscible flooding of petroleum reservoirs by lean gas, carbon dioxide, natural gas, and other high pressure injection fluids has become an economically viable technique for petroleum production. Introduction of a miscible fluid in petroleum reservoirs, will, in general, produce a number of alterations in petroleum fluid flow and phase behavior and reservoir rock characteristics. One such alteration is the heavy organic precipitation, flocculation and deposition (asphaltenes, diamondoids, etc.), which in most of the observed instances result in plugging or wettability reversal in the conduits [3-7].

In our recent reports we presented the various causes and effects of phase behavior of petroleum fluids containing heavy organic fractions and their depositions [8, 9]. It is always preferred to prevent heavy organics deposition during petroleum fluid flows. In cases when heavy organics precipitation could not be prevented we need to understand the fluid flow behavior which is less likely to cause fouling of a conduit. In these cases there is a need for understanding how the precipitated and flocculated particles suspended in the oil will behave under certain flow conditions. This motivated the research presented in this report. Our main objective is to study the behavior of suspended heavy organic particles during flow conditions.

As a preliminary step, the tendency of the crude oil to form solid particles, whenever a miscible solvent is injected into the petroleum reservoir, must be determined. This may be accomplished by using existing experimental techniques [6, 7] together with predictive models and packages [5]. These combined experimental / predictive approaches have proven to be a useful tool for design of production and transportation schemes for crude oils prune to heavy organics precipitation, flocculation and deposition.

The study of the behavior of suspended heavy-organic particles during flow conditions has been focused on the production well since flow through a pipeline is only a special case of this more general one. A typical production well may be divided into two distinct sections:

(I). The region above the bubble point (single-phase) is the emphasis of the present report. Understanding of deposition of particles in this region is especially important for particles which enter into the oil well from the reservoir.

(II). The analysis of the region below the bubble-point (two-phase flow) is the subject of our ongoing research.

In this report we present an analytical model for the heavy organic suspended particles deposition coefficient prior to deposition corresponding to petroleum fluids flow in producing wells condition. In our previous publications [3, 4, 10] we reported various segments of this analytical model some of which contained typo errors. For the sake of comprehensiveness and to provide the readership with the details of the algebraic manipulations involved we report here the details of the model in its entirety.

DEVELOPMENT OF THE ANALYTICAL MODEL

The theory presented here is for a turbulent petroleum fluid system of constant density, and viscosity. For petroleum fluid flow in wells this is the case for the region above the

bubble pressure where only the liquid phase is the medium for the suspended particles.

Substantial research work has been done on the topic of particle deposition on the walls of channels or pipes in turbulent flow by many researchers [11-17]. The model presented here is a combination of the work performed by the authors mentioned above, modified to be applicable to the deposition of heavy organic particles in turbulent petroleum fluid flow. A key assumption in the development of this model is that fully developed petroleum turbulent flow has a structure as proposed by Lin *et al*. From experimental observations, they proposed a generalized velocity distribution for turbulent flow of fluids in pipes comprised of three main regions:

- A sublaminar (wall) layer $0 \le r^* \le 5$
- A buffer layer $5 \le r^* \le 30$
- A turbulent core $30 \le r^*$

Where $r^* = D_i(V_{avg}\sqrt{f/2}/\nu)$ is a dimensionless distance measured from the wall. This dimensionless distance is a function of the inner pipe diameter, D_i, fluid average velocity, V_{avg}, the Fanning friction factor, f, and the fluid kinematic viscosity, ν. The model presented here is for a system of constant density, and viscosity. Therefore, it is applicable only to a single phase liquid petroleum fluid flow. This theory can be extended to the region below the bubble point (gas-liquid slug flow, etc.) using reliable expressions for petroleum viscosity and density versus pressure and temperature. The assumption of constant viscosity and constant density is justified since density changes are not appreciable until the bubble point pressure is reached inside the well (or tubing). It is also assumed that suspended particles are of uniform diameter, and that, due to their rather low concentration we could neglect particle-particle interactions. We assume the thickness of the boundary layer is quite small compared to the radius of the pipe as a result we can neglect the wall curvature effects in our model.

We start with reporting the equation which is used to describe the particle flux, N_P, in terms of the diffusivities and the concentration gradient [18], i.e.,

$$N_P = \left(\mathcal{D}^B + \mathcal{D}^E\right)\frac{dC^P}{dr}, \qquad (1)$$

where $\mathcal{D}^B$ is the Brownian diffusivity; $\mathcal{D}^E$ is the eddy diffusivity; C^P is the particles concentration and r is the radial distance. The Brownian diffusivity is defined by the following equation

$$\mathcal{D}^B = \frac{k_B T}{3\pi . d_P . \mu} \qquad (2)$$

where k_B is the Boltzmann constant (k_B=1.38066x10^{23} [J/K]); T is the absolute temperature; d_P is the particle diameter and μ is the liquid viscosity of the suspending medium (petroleum fluid). Equation (1) is subject to the boundary condition:

at $r = S_d$ $\quad C^P = C^P_{Sd}$,

where C^P_{Sd} is the particle concentration at r = S_d and S_d is the particle "stopping distance" measured from the wall. A particle needs to diffuse only within one stopping distance from the wall, and from this point on, due to the particle momentum, it would coast to the wall. For small particles the stopping distance is small compared with the boundary layer thickness and consequently diffusion dominates. The proposed correlation for the particle stopping distance is [13]:

$$S_d = \frac{0.05\rho_P V_{avg} d_P^2 \sqrt{f/2}}{\mu} + \frac{d_P}{2}, \qquad (3)$$

where ρ_P is density of particles; V_{avg} is the petroleum fluid average velocity and f is the Fanning friction factor. Equation (1) may be integrated following the procedure for the calculation of temperature drop across a composite wall. We will find the concentration profiles from point to point across the boundary layer. That is, we will calculate the concentration differences through the sublaminar layer, the buffer region and the turbulent core. By adding these concentration differences we can find the overall particle flux in terms of the average and wall concentrations. Before we integrate equation (1) for C^P, we need to have expressions for N_P and $\mathcal{D}^E$ as functions of the radial distance (r) for each of the three main regions in the oil well and pipeline, i.e. sublaminar layer, buffer layer and turbulent core.

1. Sublaminar Layer

Johansen [17] proposed the following correlation to express the eddy diffusivity as a function of radial distance (r) for the sublaminar layer:

$$\mathcal{D}^E = \nu\left(\frac{r^*}{11.15}\right)^3 \text{ for } r^* \le 5 \quad \text{or} \quad \frac{\mathcal{D}^E_{*_{s_d-5}}}{\nu} = \left(\frac{r^*}{11.15}\right)^3 \qquad (4)$$

In this equation ν is the kinematic viscosity of the flowing petroleum fluid, r* is the dimensionless radial distance and $\mathcal{D}^E_{*_{s_d-5}}$ represents the sublaminar layer ($r^* \le 5$) eddy diffusivity,

The particle molar flux, N_P, is assumed to vary linearly from the wall to the center line of the channel, as proposed by Beal [14]:

$$N^P = N^P_o\left(1 - \frac{2r^*}{D^*_i}\right) \qquad (5)$$

In this equation N^P_o is the particle flux at the wall; r^* is a dimensionless radial distance and D^*_i is the dimensionless inner well (or tubing) diameter, both defined by the following equations

$$r^* = r\left[\frac{V_{avg}\sqrt{f/2}}{\nu}\right] \qquad (6)$$

$$D_i^* = D_i\left[\frac{V_{avg}\sqrt{f/2}}{\nu}\right] \tag{7}$$

Where D_i is the inner diameter of the well (or tubing), V_{avg} is the fluid average velocity, f is the Fanning friction factor and ν [m^2/s] is kinematic viscosity of the flowing fluid. Let us also define the dimensionless stopping-distance, s_d^* by the following equation

$$s_d^* = s_d\left[\frac{V_{avg}\sqrt{f/2}}{\nu}\right]. \tag{8}$$

For the sublaminar layer Equation (1) may be integrated following the procedure for the calculation of temperature drop across a composite wall. We will find the concentration profiles from point to point across the boundary layer. That is, we will calculate the concentration differences through the sublaminar layer, the buffer region and the turbulent core. By adding these concentration differences we can find the overall particle flux in terms of the average and wall concentrations. Note that Equation (4) is only valid for dimensionless radial distances smaller than 5, which is the limit of the sublaminar layer.

Introducing all the new dimensionless variables and the expressions for N and $\mathcal{D}^E$ into Equation (1), considering that $dr = dr^*\left[\frac{\nu}{V_{avg}\sqrt{f/2}}\right]$ we get:

$$N_P = N_o^P\left(1-\frac{2r^*}{D_i^*}\right) = \left[\frac{\mathcal{D}^B}{\nu}+\left(\frac{r^*}{11.15}\right)^3\right]V_{avg}\sqrt{f/2}\,\frac{dC^P}{dr^*}, \tag{9}$$

subject to the following boundary conditions:

$$\begin{cases} \text{at } r^* = S_d \;\; C^P = C^P_{S_d^*} \\ \text{at } r^* = 5 \;\; C^P = C_5^P \end{cases}$$

Rearranging Equation (9), integrating and applying the above boundary conditions we arrive at the following integral form:

$$C_5^P - C^P_{S_d^*} = \frac{N^P_{\,0}}{V_{avg}\sqrt{f/2}}\left[\frac{11.15N_{Sch}^{2/3}}{3}F_1 - \frac{2(11.15)^2 N_{Sch}^{1/3}}{3D_i^*}F_2\right] \tag{10}$$

In the above equation N_{Sch} is the Schmidt Number defined as

$$N_{Sch} \equiv \frac{\nu}{\mathcal{D}^B}, \tag{11}$$

and F_1 and F_2 are defined by the following expressions,

$$F_1 = \frac{1}{2}\ln\left[\frac{(1+5\varphi)^2}{(1-5\varphi)^2}\right] - \frac{1}{2}\ln\left[\frac{(1+s_d^*\varphi)^2}{(1-s_d^*\varphi)^2}\right] + \sqrt{3}\tan^{-1}\left(\frac{10\varphi-1}{\sqrt{3}}\right) - \sqrt{3}\tan^{-1}\left(\frac{2s_d^*\varphi-1}{\sqrt{3}}\right), \tag{12}$$

$$F_2 = \frac{1}{2}\ln\left[\frac{(1-5\varphi)^2}{(1+5\varphi)^2}\right] - \frac{1}{2}\ln\left[\frac{\left(1-s_d^*\varphi\right)^2}{\left(1+s_d^*\varphi\right)^2}\right] + \sqrt{3}\tan^{-1}\left(\frac{10\varphi-1}{\sqrt{3}}\right) - \sqrt{3}\tan^{-1}\left(\frac{2s_d^*\varphi-1}{\sqrt{3}}\right), \qquad (13)$$

where for simplicity we have defined

$$\varphi \equiv \frac{N_{Sch}^{1/3}}{11.15}. \qquad (14)$$

Equations (10-14) describe the transport of suspended particles in the sublaminar layer to the wall in terms of the concentration difference between the limits $r^* = S_d^*$ (dimensionless stopping distance) and $r^* = 5$ (limit of the sublaminar layer).

2. Buffer Layer

The next step is the calculation of the particle flux between the concentration at $r^* = 5$ and $r^* = 30$ (limit of the buffer layer). The eddy diffusivity expression for the buffer layer is assumed to be:

$$\mathcal{D}^E = \nu\left(\frac{r^*}{11.4}\right)^2 - 0.1923 \text{ for } 5 \le r^* \le 30 \quad \text{or} \quad \frac{\mathcal{D}^E_{s_d^*-30}}{\nu} = \left(\frac{r^*}{11.4}\right)^2 - 0.1923 \qquad (15)$$

Integration of Equation (1), using Equation (15) for $\mathcal{D}^E_{s_d^*-30}$ gives:

$$C^P_{30} - C^P_5 = \frac{N^P_o}{V_{avg}\sqrt{f/2}}\left[11.4\theta \cdot F_3\right] - \frac{11.4^2}{D_i^*}\ln\left[\frac{11.4^2-(30\theta)^2}{11.4^2-(5\theta)^2}\right], \qquad (16)$$

where,

$$F_3 = \frac{1}{2}\ln\left[\frac{11.4-30\theta}{11.4+30\theta}\right] - \frac{1}{2}\ln\left[\frac{11.4-5\theta}{11.4+5\theta}\right], \qquad (17)$$

and

$$\theta \equiv \left[\frac{N_{Sch}}{(0.1923\cdot N_{Sch}-1)}\right]^{1/2}. \qquad (18)$$

Equation (16) describes the particle transport in terms of the concentration difference between the limits of the buffer layer.

3. Turbulent Core

The following step is the calculation of the particle transport rate in the turbulent core in terms of the difference between the concentration at r* = 30 (upper limit of the buffer layer) and the bulk concentration (average conc.). The eddy diffusivity for the turbulent core is taken to be [17]:

$$\mathcal{D}^E = 0.4 r^* . \nu \quad \text{for} \quad r^* \geq 30 \quad \text{or} \quad \frac{\mathcal{D}^E_{30-avg}}{\nu} = 0.4 r^* . \tag{19}$$

If we assume that at $V=V_{avg}$ we have $C^P = C^P_{avg}$, then we could integrate Equation (1) using Equation (19) to obtain the following expression for C^P_{avg},

$$C^P_{avg} - C^P_{30} = \frac{N^P_o}{V_{avg}\sqrt{f/2}} \left\{ \left(2.5 + \frac{12.5}{D^*_i N_{Sch}} \right) \ln \left(\frac{1 + 0.4 r^*_{avg} N_{Sch}}{1 + 0.4 r^* N_{Sch}} \right) - \frac{5 r^*_{avg}}{D^*_i} + \frac{5 r^*}{D^*_i} \right\} \tag{20}$$

In this expression r^*_{avg} is the dimensionless radial distance (measured from the wall) where $V=V_{avg}$. Equation (20) describes the particle transport in terms of the concentration difference between the bulk (average) and the upper limit of the buffer layer.

So far, we have expressions for the three different regions (sublaminar/wall layer, buffer layer, and turbulent core). Now they may be added together to obtain an expression for N_o in terms of $C^P_{avg}, C^*_{S_d}$, average fluid velocity, S^*_d, and physical parameters of the system.

Until now, only dimensionless stopping distances (S^*_d) with values less than 5 have been considered. However, for particles large enough S^*_d could be greater than 5. If so, then the preceding analysis is not valid under these conditions. This difficulty may be overcome if Equation (1) is integrated between the limits

$C^P = C^P_{S^*_d}$ at $r^* = S^*_d$,

and

$C^P = C^P_{30}$ at $r^* = 30$,

using the eddy diffusivity correlation for the buffer layer as expressed by equation (15).

Introducing Equation (15) into Equation (1) and integrating using the assumptions noted previously, we get:

$$C^P_{30} - C^P_{S^*_d} = \frac{11.4 N_0}{V_{avg}\sqrt{f/2}} \left\{ \theta . F_4 - \frac{11.4}{D^*_i} \ln \left[\frac{11.4^2 - (30\theta)^2}{11.4^2 - (s^+\theta)^2} \right] \right\}, \tag{21}$$

Such that,

$$F_4 = \frac{1}{2} \ln \left[\frac{11.4 - 30.\theta}{11.4 + 30.\theta} \right] - \frac{1}{2} \ln \left[\frac{11.4 - s^*_d \theta}{11.4 + s^*_d \theta} \right], \tag{22}$$

and θ is defined by Eq. (18).

For S_d^* =5 then Equations (21) and (22) reduce to equation (16) and (17). Equation (13) still applies to the turbulent core.

For particles with a dimensionless stopping distance 0 ≤ S_d^* < 5:

We add equations (10), (16), and (20), to obtain an expression for the mass transfer (transport) coefficient defined as $N_o^P/(C_{avg}^P - C_{s_d^*}^P)$ = K with the dimension of velocity [cm/sec]. The expression for the deposition coefficient obtained is:

$$K = V_{avg}\sqrt{f/2}\left\{\frac{11.15^3\varphi^2}{3}F_1 - \frac{11.15^3\varphi}{1.5D_i^*}F_2 + 11.4\theta.F_3 + F_5\right\}^{-1} \quad (23)$$

Parameter F_1, F_2 and F_3 appearing in this equation are the same as defined previously by Equations (12), (13) and (17), respectively and parameter F_5 is given below:

$$F_5 = -\frac{11.4^2}{D_i^*}\ln\left[\frac{11.4^2-(30\theta)^2}{11.4^2-(5\theta)^2}\right] + \left(2.5 + \frac{12.5}{D_i^* 11.15^2\varphi^2}\right)\ln\left[\frac{1+0.4(11.15^2)r_{avg}^*\varphi^2}{1+12(11.15^2)\varphi^2}\right] + \frac{150 - 5r_{avg}^*}{D_i^*} \quad (24).$$

For particles with a dimensionless stopping distance 5 ≤ S_d^* < 30:

By combining Equations (20) and (21) and solving for K we get:

$$K = V_{avg}\sqrt{f/2}\,/\{11.4\theta.F_4 + F_5\} \quad (25)$$

Parameters F_4 and F_5 appearing in this equation are the same as previously defined by Equations (22) and (24), respectively.

Inertial Effects

In the above analysis we have derived analytical expressions for the mass deposition coefficient for different particle sizes in terms of the dimensionless stopping distance S_d^*. Next we must account for the inertial effects. We use the following expression to account for inertial effects [14]:

$$K^{iner} = \frac{N_o^P}{C_{avs}^P} = \frac{K.p.\vartheta}{K + p.\vartheta}, \quad (26)$$

where K^{iner} is the deposition coefficient (mass transfer coefficient which contains the inertial effects), N_o^P is particle flux at the wall (as previously defined); p is the particle sticking factor (taken equal to unity); ϑ is the average velocity of the particles near the walls, and it consists of two parts:

$$\vartheta = \vartheta_{\mathrm{fm}} + \vartheta^{\mathrm{B}}, \tag{27}$$

where ϑ_{fm} is the particle velocity component due to fluid motion and ϑ^{B} is the component due to particle Brownian motion,

$$\vartheta^{\mathrm{B}} = \left(\frac{\mathrm{k_B T}}{3\pi.\mathrm{m}}\right)^{1/2}, \qquad \mathrm{k_B} = \frac{1}{4}\mathrm{V_{avg}}\sqrt{\mathrm{f}/2}\left(\vartheta^{*}_{fm}(\mathrm{d}^{*}/2) + \vartheta^{*}_{fm}(\mathrm{S}^{*}_{\mathrm{d}})\right), \tag{28}$$

and where m is the particle mass, $\vartheta^{*}_{fm}(\mathrm{d}^{*}/2)$ is the particle velocity at a dimensionless radial distance $\mathrm{d}^{*}/2$, d^{*} is the dimensionless particle diameter, and $\vartheta^{*}_{fm}(\mathrm{S}^{*}_{\mathrm{d}})$ is the particle velocity at a dimensionless radial distance $\mathrm{S}^{*}_{\mathrm{d}}$ (dimensionless stopping distance). The quantity ϑ^{*}_{fm} can be calculated using the following correlation proposed by Laufer, (1954):

$\vartheta^{*}_{fm} = 0.05\mathrm{r}^{*}$ for $0 \le \mathrm{r}^{*} \le 10$

$\vartheta^{*}_{fm} = 0.5 + 0.0125\,(\mathrm{r}^{*} - 10)$ for $10 \le \mathrm{r}^{*} \le 30$

The particles can be anywhere between $\mathrm{r}^{*} = \mathrm{d}^{*}/2$ and $\mathrm{r}^{*} = \mathrm{S}^{*}_{\mathrm{d}}$. Considering this we are to choose the appropriate expression for ϑ^{*}_{fm}.

The analysis for particle deposition onto the walls of a flowing channel from turbulent fluid streams is concluded by taking into account the inertial effects as in Equation (25). At this point all the phenomena influencing the deposition rate (Brownian diffusivity, eddy diffusivity, and inertial effects) have been taken into account.

PREDICTIONS FOR PARTICLE DEPOSITION IN WELLS AND TUBINGS

In our previous publications [3, 4, 10] we compared the predictions of the proposed model with the available experimental data and the other models. Since experimental data for particle deposition from turbulent petroleum fluid flows was scarce we used the deposition data from aerosols to verify our model. As it was shown, the results of our analysis for particle deposition from turbulent fluid streams were in very good agreement with the experimental deposition rates for aluminum and iron particles in air. The predictions of the present model showed a better agreement with the mentioned experimental data than the models proposed earlier. We believe our model is suitable for *a priori* predictions of the particle deposition coefficient from turbulent petroleum fluid flow.

Figure 2(left) shows the predicted deposition coefficients for particles as a function of particle diameter suspended in a light petroleum fluid with 30.21 °API gravity (corresponding to 0.875 SG) and the kinematic viscosity of 11 centi-Stokes (cSt) at various production rates. Figure 2(right) shows the predicted deposition coefficients values for petroleum fluids with different kinematic viscosities (and at different °APIs)

and containing suspended particles of 1,000 nm in diameter.

The particle sizes analyzed ranged from 5 to 200,000 nm. According to Figure 2(left) deposition coefficients are generally small except at high production rates and for very large particles. Note a minimum after which the deposition coefficient increases more rapidly with increasing particle diameter. This is due to the fact that at the minimum point the deposition process is momentum controlled. According to Figure 2(left), particle deposition from turbulent petroleum fluid flow is very small when the diameter of the suspended particles is less than 1,000 nm. Figure 2(right) indicates a decrease in the deposition coefficients with increasing kinematic viscosity and an increase in the deposition coefficient with increasing production rate. The lighter the petroleum fluid the higher the probability of having particle deposition.

Figure 3 shows the predicted deposition coefficients for particles as a function of the crude oil production rate for two extreme particles sizes, 3.5 nm (corresponding to asphaltene steric-colloidal particles in original crude oil) and 270 nm (corresponding to flocculated asphaltene aggregates). As it was mentioned the present analysis is for the single-phase region of the well-tubing (region before the bubble point is reached). One can notice from this figure the very small values of deposition coefficients for 3.5 nm size particles, for the volumetric flow rates of up to 3,000 cu.m/day. Figure 3 also indicates that deposition coefficients increase with increasing velocities. However, when the oil production rate is about 10,000 m^3/day, deposition coefficient is roughly 0.06 cm/min. Therefore we would expect sizeable amounts of deposition at high production rates.

With the idea in mind of finding another factor that could increase the particles tendency to deposit, we examined the effect of particle size on deposition coefficient. This is shown in Figure 4 where we can notice that deposition coefficients decrease with increasing particle size due to the fact that Brownian diffusion is inversely proportional to the particle size of the diffusing species. However, with increasing particle size (or mass) the momentum increases, so that particle momentum effects become more important. It is expected a minimum deposition rate for a given particle size, beyond which the process is essentially momentum controlled, resulting in higher deposition rates. For a radius of 270 nm, we still notice very small values (see figure 3), this means that heavy organic particle size must become much larger in order to exhibit high deposition rates.

We performed model predictions varying the kinematic viscosity of the crude oil to study the effect of this parameter on the deposition coefficient. This was done because kinematic viscosity decreases with increasing temperature, and because it is a function of the API gravity of the crude oil. Figure 5 shows the predicted values, and we can see a decrease in the deposition coefficient with increasing kinematic viscosity. This means that the lighter the petroleum fluid is the higher the probability of having heavy organic deposition will be. However, these predicted values are still very small.

CONCLUSIONS

The model developed for the particle deposition onto the walls of a pipe from a turbulent petroleum fluid stream in oil wells and pipelines is used to predict the deposition coefficient from turbulent flow production operations. The effect of particle size on the deposition coefficient was investigated, finding that when the deposition process is

diffusion-controlled (particles with diameter < 1,000 nm) the predicted values are very small. However, when the deposition process is momentum controlled (particles with diameters > 1,000 nm) the predicted values for the deposition coefficient increase more rapidly with increasing particle diameter. We also investigated the effect of petroleum fluid kinematic viscosity on the deposition coefficient. We found that the deposition coefficient decreases with increasing petroleum fluid kinematic viscosity. For kinematic viscosity of 12.16 cSt the predicted deposition coefficient is negligible for suspended particles of 1,000 nm. We also found that the deposition coefficient increases with increasing production rate. This is due to the fact that at larger production rates the amount of eddy diffusion is bigger. The proposed model can be used for various cases of the behavior of heavy organics particle depositions from turbulent petroleum flows so long as the particles are neutral, their sizes are stable, there are no particle-particle interactions and there are no phase transitions occurring in the flow. However, in cases where such changes are occurring in the system this model will require appropriate modifications as presented and applied elsewhere [19].

Acknowledgements: The authors would like to thank Aly Hamouda, Diogo Melo Paes, Paulo Ribeiro, Kamy Sepehrnouri and Mahdy Shirdel for taking time to read the manuscript and suggesting very useful corrections. To receive the executable computer package and the set of related equation for our proposed model please contact the corresponding author.

Nomenclature

C^P	Particles concentration
d_P	Particle diameter
$\mathcal{D}^B$	Brownian diffusivity
$\mathcal{D}^E$	Eddy diffusivity
$\mathcal{D}^E_{s_d^*-5}$	Sublaminar layer ($r^* \leq 5$) eddy diffusivity
$\mathcal{D}^E_{s_d^*-30}$	Buffer layer ($5 \leq r^* \leq 30$) eddy diffusivity
$\mathcal{D}^E_{30-avg}$	Turbulent core ($30 \leq r^*$) eddy diffusivity
D_i	Inner diameter of well (or tubing)
D_i^*	$= D_i.V_{avg}\sqrt{f/2}/\nu$ Dimensionless inner diameter of well (or tubing)
f	Friction factor
k_B	Boltzmann constant (K_B=1.38066x10^{23} [J/K])
N_P	Particle flux
N_o^P	Particle flux at the wall
r	Radial distance
r*	$= r.V_{avg}\sqrt{f/2}/\nu$ Dimensionless radial distance
S_d	Particle "stopping distance" measured from the wall
S_d^*	$= S_d.V_{avg}\sqrt{f/2}/\nu$
T	Absolute temperature
V_{avg}	Fluid average velocity
μ	Petroleum fluid viscosity
ν	Kinematic viscosity (ν= μ/ρ) [m^2/s]

ρ_P Density of particles

References

1. Mansoori GA, Asphaltene Deposition: An Economic Challenge in Heavy Petroleum Crude Utilization and Processing, OPEC Review, 103-113, 1988.

2. Carpentier B, Wilhelms A and Mansoori GA, Reservoir organic geochemistry: Processes and applications, J. Petrol. Sci. &
Eng., Volume 58, Issues 3-4, 2007.

3. Escobedo J and Mansoori GA, Asphaltene and Other Heavy-Organic Particle Deposition During Transfer and Production Operations, SPE paper #30672, Proceed Soc of Petrol Eng Annual Tech Conf held in Dallas TX 22-25 October 1995.

4. Escobedo J and Mansoori GA, Solid Particle Deposition During Turbulent Flow Production Operations, SPE paper #29488, Proceed Soc Petrol Eng Production Operation Symp held in Oklahoma City OK 2-4 April 1995.

5. Branco VAM, Mansoori GA, De Almeida Xavier LC, Park SJ and Manafi H, Asphaltene flocculation and collapse from petroleum fluids, J Petrol Sci & Eng 32, 217-230, 2001.

6. Mousavi-Dehghani SA, Riazi MR, Vafaie-Sefti M and Mansoori GA, An analysis of methods for determination of onsets of asphaltene phase separations, J Petrol Sci & Eng, 42 (2-4): 145-156, 2004.

7. Mansoori GA, Vazquez D and Shariaty-Niassar M, Polydispersity of heavy organics in crude oils and their role in oil well fouling, J Petrol Sci and Eng., 58(3-4), 375-390, 2007.

8. Mansoori GA, PHASE BEHAVIOR IN PETROLEUM FLUIDS, Petroleum Engineering – Downstream section of Encyclopedia of Life Support Systems, 33 pages, UNESCO, UN, Paris, France, 2009.

9. . Mansoori GA, A unified perspective on the phase behaviour of petroleum fluids,, Int. J. Oil, Gas and Coal Technology 2(2) 141-167, 2009.

10. Escobedo J and Mansoori GA, Prefouling Behavior of Suspended Particles in Petroleum Fluid Flow, Scientia Ir., Transactions C: Chemistry and Chemical Engineering 17, (to appear), 2010.

11. Lin CS, Moulton RW and Putnam GL, Mass transfer between solid wall and fluid streams, Ind Eng Chem 45, pp.636-646 (1953).

12. Lauufer J, The Structure of Turbulence in Fully developed pipe flow, NACA 1174, National Advisory Committee for Aeronautics, 1954. (Available from NASA as TR-1174).

13. Friedlander SK and Johnstone HF, Deposition of suspended particles from turbulent gas streams, Ind Eng Chem 49(7) 1151-1156, July 1957.

14. Beal SK, Deposition of particles in turbulent flow on channel or pipe walls, Nuclear Sci Eng 40, 1-11, 1970.

15. Chen SK and Ahmadi G, Deposition of particles in a turbulent pipe flow, Journal of Aerosol Science 28(5) 789-796, 1997.

16. Derevich IV and Zaichik LI, Particle deposition from a turbulent flow, Fluid Dynamics, 23(5) 722-729, 1988.

17. Johansen ST, The Deposition of Particles on Vertical Walls, Int J Multiphase flow 17(3) 355-362,1991.

18. Von Karman T, Aerodynamics: Selected Topics in the Light of Their Historical Development, www.doverpublications.com, 2004.

19. Mansoori GA, ASPHRAC: A comprehensive package of computer programs and database which calculates various properties of petroleum fluids containing heavy organics: www.uic.edu/~mansoori/ASPHRAC_html

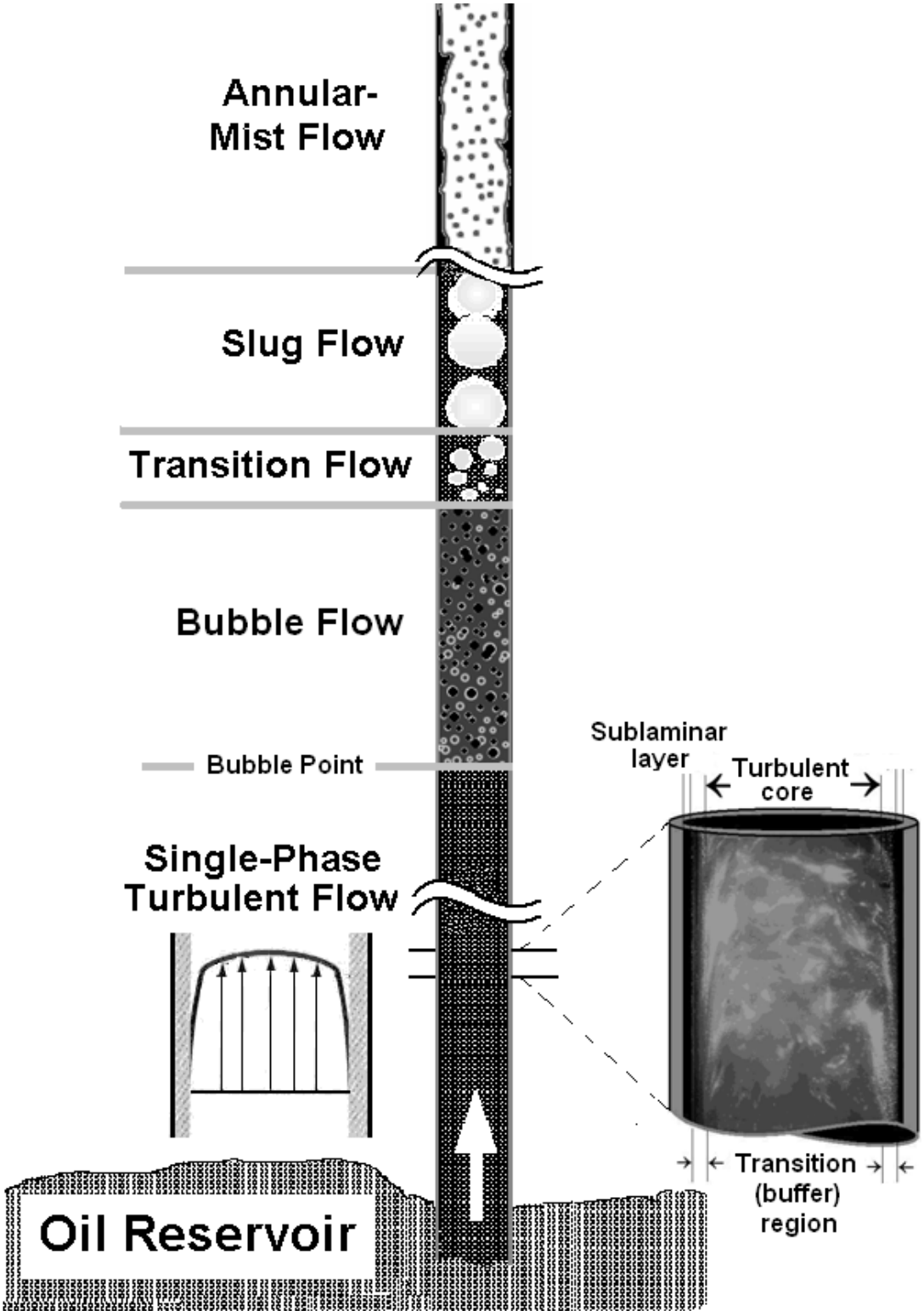

Figure 1 – *Illustration of velocity distribution and different flow regimes in the prefouling single-phase turbulent flow condition in the oil well.*

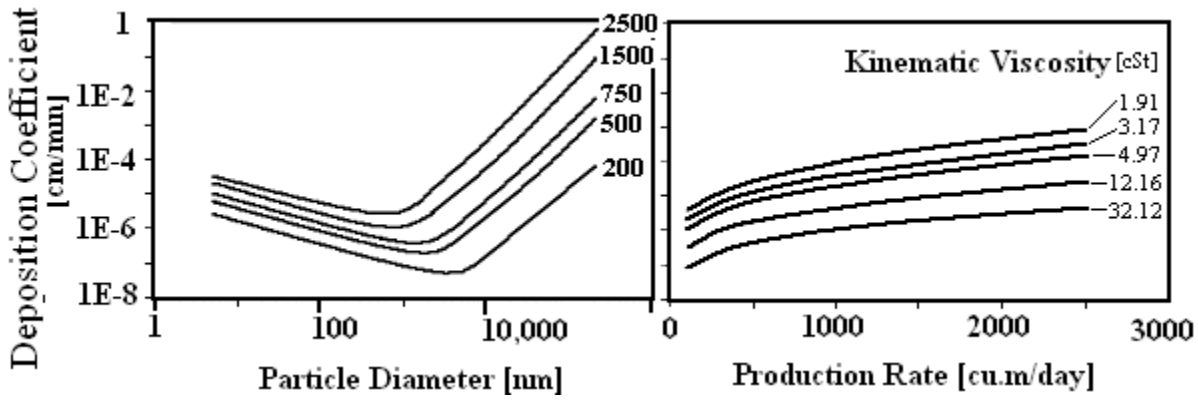

Figure 2 – (Left Figure) Effect of particle size on the deposition coefficient for a 30.21 °API petroleum fluid with a kinematic viscosity of 11 cSt at various production rates in (cu.m/day]. (Right Figure) Effect of petroleum production rate on the deposition coefficient of 1 micron (1000 nm) in diameter suspended particles in petroleum fluids of various kinematic viscosities ranging from 1.91 - 32.12 cSt.

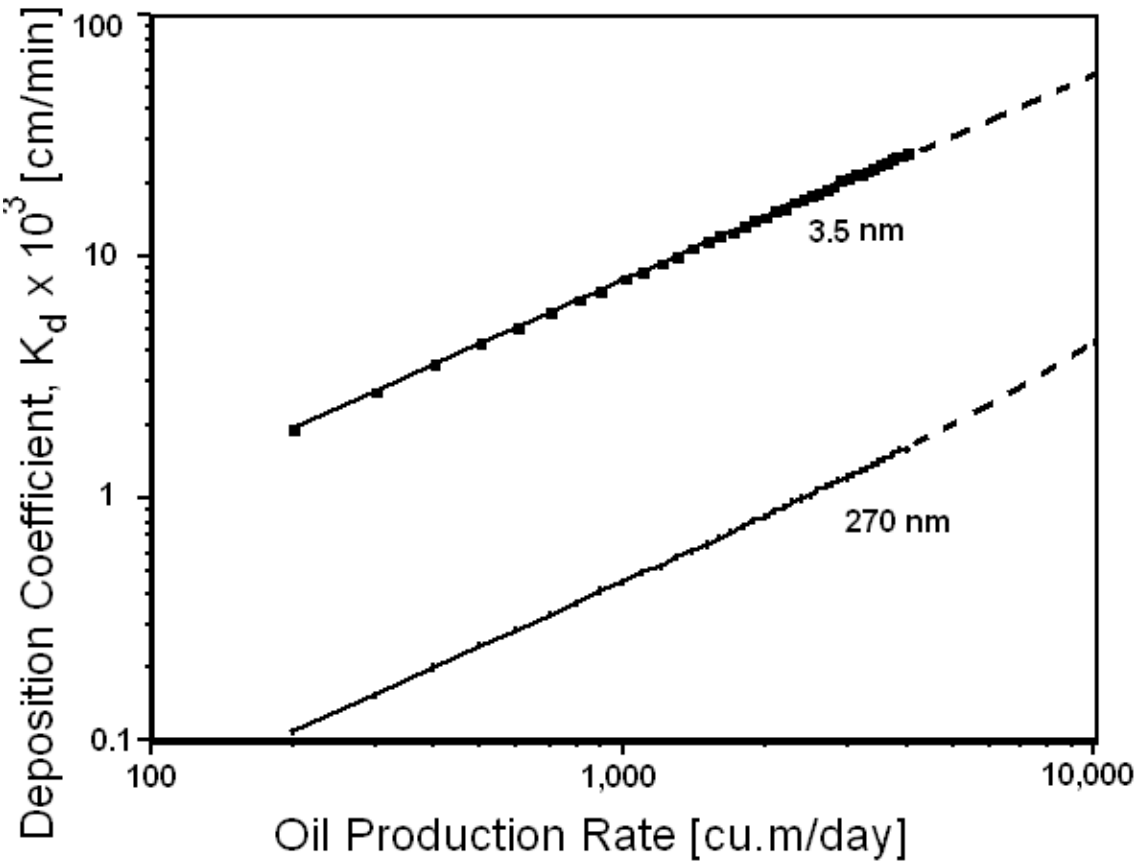

Figure 3. Predicted deposition coefficients as a function of the crude oil production rates. It is calculated for particles with a diameter of 3.5 nm suspended in a 37.8 ^{o}API petroleum fluid.

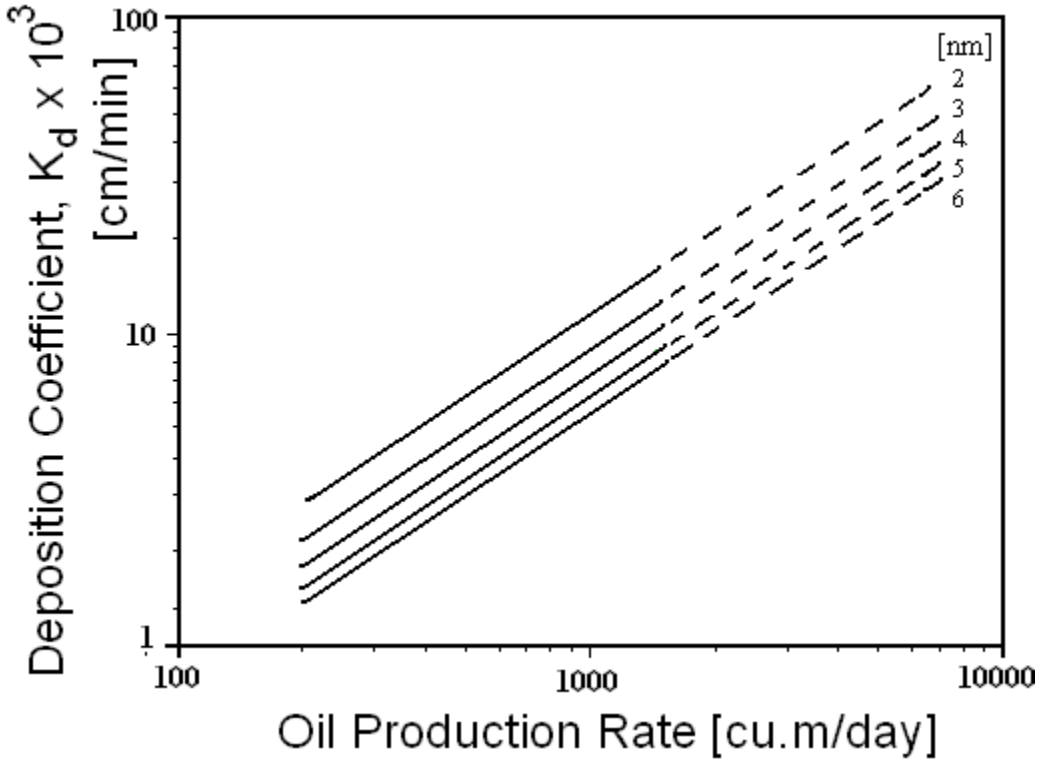

Figure 4. Effect of particle size on deposition coefficient for a 37.8 ^{o}API petroleum fluid.

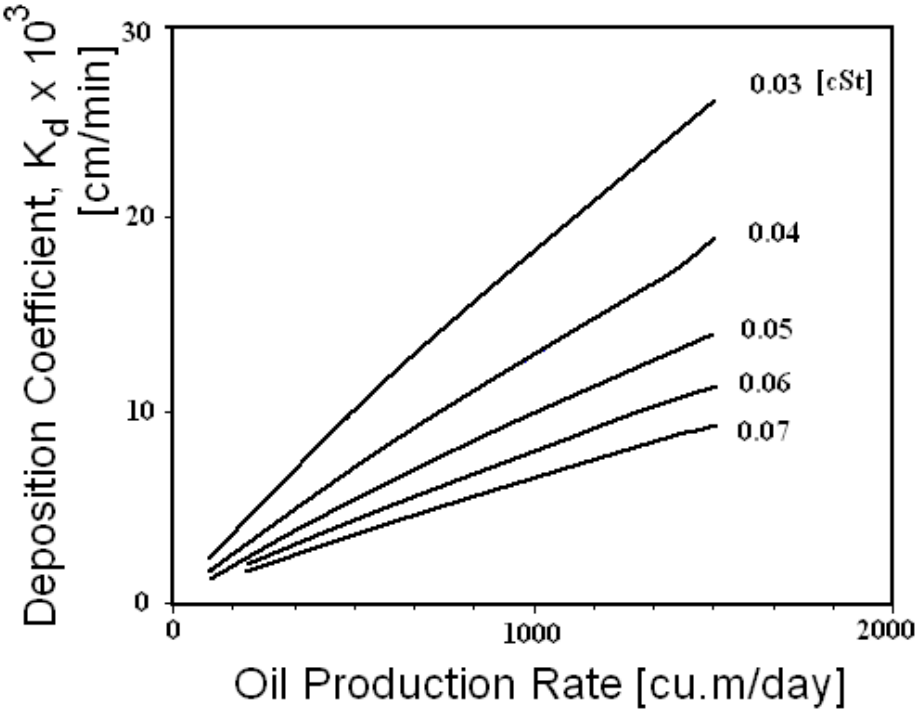

Figure 5. Effect of kinematic viscosity on deposition coefficient.